## $B \to K \nu \bar{\nu}$ , MiniBooNE and muon g-2 anomalies from a dark sector

Alakabha Datta, <sup>1,2,3,\*</sup> Danny Marfatia, <sup>4,†</sup> and Lopamudra Mukherjee <sup>5,‡</sup>

<sup>1</sup>Department of Physics and Astronomy, University of Mississippi,

108 Lewis Hall, Oxford, Mississippi 38677, USA

<sup>2</sup>SLAC National Accelerator Laboratory, 2575 Sand Hill Road, Menlo Park, California 94025, USA

<sup>3</sup>Santa Cruz Institute for Particle Physics, Santa Cruz, California 95064, USA

<sup>4</sup>Department of Physics and Astronomy, University of Hawaii, Honolulu, Hawaii 96822, USA

<sup>5</sup>School of Physics, Nankai University, Tianjin 300071, China

(Received 26 October 2023; accepted 13 January 2024; published 15 February 2024)

Belle II has reported the first evidence for  $B^+ \to K^+ \nu \bar{\nu}$  with a branching ratio  $2.7\sigma$  higher than the standard model expectation. We explain this and the MiniBooNE and muon anomalous magnetic moment anomalies in a model with a dark scalar that couples to a slightly heavier sterile Dirac neutrino and that communicates with the visible sector via a Higgs portal. We make predictions for rare kaon and other B meson decays.

DOI: 10.1103/PhysRevD.109.L031701

Introduction. Anomalies in the charged and neutral current B decays have been an active area of research for almost a decade. The recently updated measured values of  $R_{K^{(*)}}$  $\mathcal{B}(B \to K^{(*)} \mu^+ \mu^-) / \mathcal{B}(B \to K^{(*)} e^+ e^-)$  are now fully consistent with the standard model (SM) expectation [1], and have dampened interest in neutral current (NC) B anomalies (although the individual branching fractions remain discrepant [2]). However, a first measurement by Belle II of the branching ratio  $\mathcal{B}(B^+ \to K^+ \nu \bar{\nu}) = (2.3 \pm 0.7) \times 10^{-5}$ [3] is  $2.7\sigma$  higher than the SM expectation  $\mathcal{B}(B^+ \to SM)$  $(K^+ \nu \bar{\nu})_{SM} = (5.58 \pm 0.38) \times 10^{-6}$  [4] and has revived interest in NC B decays [5–10]; an earlier upper limit by Belle II [11] also led to a flurry of theoretical activity [12–17]. Unlike the dilepton modes in  $R_{K^{(*)}}$ , the contamination from  $c\bar{c}$  states in  $B \to K^{(*)} \nu \bar{\nu}$  can be neglected. Hence, if confirmed, the Belle II result could be a clear sign of new physics. Note that any theoretical interpretation must be compatible with constraints on the other  $B \to K^* \nu \bar{\nu}$ decays in Table I.

Decays of B mesons that involve invisible final states are excellent probes of new invisible or long-lived states like a massive sterile neutrino  $\nu_D$ . These states may be produced via mixing with the active neutrinos or through new

Published by the American Physical Society under the terms of the Creative Commons Attribution 4.0 International license. Further distribution of this work must maintain attribution to the author(s) and the published article's title, journal citation, and DOI. Funded by SCOAP<sup>3</sup>. mediators such as new vector bosons or leptoquarks that couple them to SM particles. We consider a mechanism in which  $\nu_D$  communicates with the SM sector through a light scalar mediator S [37] that couples to the SM sector through an extended Higgs portal [38–40]. The scalar couples to active neutrinos via four-neutrino mixing and a contribution to  $B^+ \to K^+ \nu \bar{\nu}$  is generated by the two body decays,  $B^+ \to K^+ S$  and  $S \to \nu \bar{\nu}$ .

Our framework also permits an understanding of the excess in electronlike events in the MiniBooNE experiment [41] in terms of a light neutrino upscattering into  $\nu_D$  which subsequently decays to  $\nu S(\rightarrow e^+e^-, \gamma\gamma)$ . Note that similar upscattering into  $\nu_D$  via a dark vector boson Z' [42,43] is excluded [44] by data from the CHARM-II [45] and MINERvA [46] experiments if the Z' is lighter than the sterile neutrino as in Ref. [42]. As shown in Ref. [37], with a light scalar mediator, the solution to the MiniBooNE anomaly is consistent with the CHARM-II and MINERvA data even with S lighter than the sterile neutrino. It is noteworthy that this explanation is untested by the template analysis of MicroBooNE [47].

Another long-standing anomaly is that of the anomalous magnetic moment of the muon,  $a_{\mu} \equiv (g-2)_{\mu}/2$ . The SM prediction [35] is more than  $5\sigma$  smaller than the updated world average following the latest experimental measurement [36],

$$\Delta a_{\mu} = a_{\mu}^{\text{exp}} - a_{\mu}^{\text{SM}} = (2.49 \pm 0.48) \times 10^{-9}.$$
 (1)

The anomaly can be resolved by including a higher-dimensional coupling to two photons [37,39]. This coupling can also help explain the MiniBooNE anomaly because it enables the scalar to decay to photon pairs that can be misidentified as electron events at MiniBooNE.

<sup>\*</sup>datta@phy.olemiss.edu

dmarf8@hawaii.edu

<sup>‡</sup>lopamudra.physics@gmail.com

	* **			
Observable	SM expectation	Measurement or constraint		
$\mathcal{B}(B^+  o K^+  u \bar{ u})$	$(5.58 \pm 0.38) \times 10^{-6}$ [4]	$(2.3 \pm 0.7) \times 10^{-5}$ [3]		
${\cal B}(B^0 o K^{*0} uar u)$	$(9.2 \pm 1.0) \times 10^{-6}$ [18]	$<1.8 \times 10^{-5}$ [19]		
$\mathcal{B}(B^+ \to K^{*+} \nu \bar{\nu})$	$\mathcal{B}(B^0 \to K^{*0} \nu \bar{\nu}) \frac{\tau_{B^+}}{\tau_{\nu 0}} [18]$	$<4 \times 10^{-5}$ [20]		
$\mathcal{B}(B^0 \to K^{*0} e^+ e^-)_{0.03-1 \text{ GeV}}$	$(2.43^{+0.66}_{-0.47}) \times 10^{-7}$ [21]	$(3.1^{+0.9+0.2}_{-0.8-0.3} \pm 0.2) \times 10^{-7}$ [22]		
$\mathcal{B}(B_s  o \gamma \gamma)$	$5 \times 10^{-7}$ [23]	$<3.1 \times 10^{-6}$ [24]		
$\mathcal{B}(B_s  o \mu^+\mu^-)$	$(3.57 \pm 0.17) \times 10^{-9}$ [25]	$(3.52^{+0.32}_{-0.31}) \times 10^{-9}$ [26]		
$\mathcal{B}(K_L  o \pi^0  u \bar{ u})$	$(3.4 \pm 0.6) \times 10^{-11}$ [27]	$<4.9 \times 10^{-9}$ [28]		
$\mathcal{B}(K_L \to \pi^0 e^+ e^-)$	$(3.2^{+1.2}_{-0.8}) \times 10^{-11}$ [29]	$<2.8 \times 10^{-10}$ [30]		
$\mathcal{B}(K_L o\pi^0\gamma\gamma)$	•••	$(1.273 \pm 0.033) \times 10^{-6}$ [31]		
$\mathcal{B}(K_S  o \pi^0 \gamma \gamma)$	• • •	$(4.9 \pm 1.8) \times 10^{-8}$ [31]		
$\mathcal{B}(K^+ o\pi^+\gamma\gamma)$	• • •	$(1.01 \pm 0.06) \times 10^{-6}$ [31]		
$\mathcal{B}(K^{\pm} \to \mu^{\pm} \nu_{\mu} e^{+} e^{-})_{m_{e^{+}e^{-}} \ge 140 \text{ MeV}}$	•••	$(7.81 \pm 0.23) \times 10^{-8}$ [32]		
$\Delta M_{B_s}$	$(18.4^{+0.7}_{-1.2}) \text{ ps}^{-1} [33]$	$(17.765 \pm 0.006) \text{ ps}^{-1} [31]$		
$\Delta M_K^{\ \ \ \ \ \ \ \ \ \ \ \ \ \ \ \ \ \ \ $	$(47 \pm 18) \times 10^8 \text{ s}^{-1} [34]$	$(52.93 \pm 0.09) \times 10^8 \text{ s}^{-1} \text{ [31]}$		
a	$116591810(43) \times 10^{-11}$ [35]	$116592059(22) \times 10^{-11}$ [36]		

TABLE I. Experimental measurements and constraints used in the analysis. The upper limits are at 90% C.L.

Model. The scalar Lagrangian is given by

$$\mathcal{L}_{S} \supset \frac{1}{2} (\partial_{\mu} S)^{2} - \frac{1}{2} m_{S}^{2} S^{2} - \eta_{d} \sum_{f=d,\ell} \frac{m_{f}}{v} \bar{f} f S$$
$$- \sum_{f=u,c,t} \eta_{f} \frac{m_{f}}{v} \bar{f} f S - g_{D} S \bar{\nu}_{D} \nu_{D} - \frac{1}{4} \kappa S F_{\mu\nu} F^{\mu\nu}, \qquad (2)$$

where  $v \simeq 246$  GeV is the Higgs vacuum expectation value, and d and  $\ell$  correspond to down-type quarks and leptons with a universal coupling  $\eta_d$  scaled by the respective SM Yukawa. The structure of the Lagrangian can arise from the mixing of a singlet scalar with the neutral components of a two Higgs doublet model [38–40]. We will, however, adopt an effective interaction in the spirit of Ref. [37] and take the couplings  $\eta_f$  of the scalar to the uptype quarks to not be flavor universal. The parameter  $\kappa$ , of inverse mass dimension, induces an  $S\gamma\gamma$  coupling that contributes to  $(g-2)_{\mu}$  via the one-loop Barr-Zee diagram [48]. [Without this higher-dimensional operator, the contributions to  $(g-2)_{\mu}$  are via the vertex correction of the  $\gamma\mu^+\mu^-$  vertex and self-energy diagrams, which are insufficient to address the anomaly [39].]

The light active neutrinos mix with the heavy sterile neutrino and induce a coupling of the dark scalar to the light neutrinos. The four flavor eigenstates  $\nu_{\alpha}$  are related to the mass eigenstates  $\nu_{i}$  by

$$\nu_{\alpha(L,R)} = \sum_{i=1}^{4} U_{\alpha i} \nu_{i(L,R)}, \qquad \alpha = e, \mu, \tau, D, \qquad (3)$$

where L, R indicate the handedness of the neutrino, and U is a  $4\times 4$  orthogonal matrix common to  $\nu_L$  and  $\nu_R$ . We take  $U_{e4}=U_{\tau 4}=0$ , which gives  $1-|U_{D4}|^2=|U_{\mu 4}|^2$  by unitarity. We require  $\nu_4$  to be a Dirac neutrino so that its

nonrelativistic decays,  $\nu_4 \rightarrow \nu S$ , are not isotropic [49], as required by MiniBooNE data. Note that the sterile neutrino will have a much shorter lifetime  $\sim |U_{\mu 4}|^{-2}$  than the scalar  $\sim |U_{\mu 4}|^{-4}$ .

The coupling of the light scalar to up-type quarks and light neutrinos yields several flavor changing neutral current transitions via the penguin loop. The rare hadronic decays in Table I provide constraints on the model.

Signals and constraints. We consider a dark scalar with mass in the range  $10 \lesssim m_S/\text{MeV} \lesssim 150$ . Since  $m_S < 2m_\mu$ , S can only decay to photons, electrons, and neutrinos, for which the decay widths are provided in the Supplemental Material [50]. Below, we discuss the phenomenological implications for several observables of interest and the constraints imposed on the model.

S decay length. We require the decay length of the dark scalar to be shorter than 0.1 mm to evade bounds from beam dump and other experiments that probe long-lived particles.

*B* and *K* meson decays. The Lagrangian in Eq. (2) induces two-body meson decays such as  $B \to K^{(*)}S$  and  $K \to \pi S$  at one loop. The flavor changing neutral current (FCNC) Lagrangian for the  $b \to s$  and  $s \to d$  transitions is given by

$$\mathcal{L}_{FCNC} = g_{bs}\bar{s}P_RbS + g_{sd}\bar{d}P_RsS, \tag{4}$$

where the effective couplings  $g_{bs}$ ,  $g_{sd}$  take the form

$$g_{bs} \approx \frac{3\sqrt{2}G_F}{16\pi^2} \frac{m_t^2 m_b}{v} \eta_t V_{tb} V_{ts}^*,$$
 (5)

and

$$g_{sd} \approx \frac{3\sqrt{2}G_F}{16\pi^2} \frac{m_t^2 m_s}{v} V_{ts} V_{td}^* \left( \eta_t + \eta_c \frac{m_c^2 V_{cs} V_{cd}^*}{m_t^2 V_{ts} V_{td}^*} \right).$$
 (6)

The rates for the two-body FCNC processes can be found in the Supplemental Material [50]. The relevant B meson form factors are taken from Refs. [58,59], while the kaon form factor  $|f_0^K(m_S^2)|^2$  is approximately unity [60]. It is important to note that  $g_{bs}$  is essentially determined by  $\eta_t$  since the contribution proportional to  $\eta_c$  is both helicity and charmmass suppressed. On the other hand, for  $g_{sd}$ , the contribution from  $\eta_c$  is only helicity suppressed and can be sizable for  $\eta_c \gg \eta_t$ .  $\mathcal{L}_{\text{FCNC}}$  also induces  $B_s$  decays to  $\gamma\gamma$ ,  $\mu^+\mu^-$ , and  $\nu\bar{\nu}$ . The most important constraints on the couplings from the flavor changing B and K transitions are as follows:

- (1) B decay width: We require  $\mathcal{B}(B \to K^{(*)}S) < 10\%$  so that it does not exceed the uncertainty in the SM prediction of the B meson width [61].
- (2)  $B \to K\nu\bar{\nu}$ : We require  $\mathcal{B}(B^+ \to K^+\nu\bar{\nu})$  to lie within  $1\sigma$  of the Belle II measurement in the first row of Table I.
- (3)  $B \to K^* \nu \bar{\nu}$ : We ensure that the upper limits on the branching fractions of the  $B \to K^*$  modes in Table I are satisfied.
- (4)  $B^0 oup K^{*0}e^+e^-$ : This decay has been measured by LHCb in the low dilepton mass region of 30–1000 MeV/ $c^2$  [22], which overlaps the mass range of the dark scalar. We therefore require the branching ratio to lie within  $1\sigma$  of the measured value.
- (5)  $B_s$  decays: We require the scalar contribution to  $B_s \to \gamma \gamma$  to remain below the upper limit placed by Belle [24] and the contribution to  $B_s \to \mu^+ \mu^-$  to remain within the  $1\sigma$  uncertainty of the measurement in Table I. We take the decay constant  $f_{B_s} = 230.3(1.3)$  MeV from Ref. [62]. An interesting signature is  $B_s \to \text{invisible}$  which is currently not constrained by experiment but can be probed at Belle II. We make predictions for its branching fraction for some benchmark points.
- (6)  $K^+ \to \pi^+ \nu \bar{\nu}$ : The NA62 experiment at CERN has set stringent limits on  $\mathcal{B}(K^+ \to \pi^+ X)$  as a function of the X mass and lifetime for invisible X decays except in the range  $110 < m_X/\text{MeV} < 160$  [63,64]. However, since S has a very short lifetime,  $\mathcal{O}(0.1)$  ps, these limits do not apply.
- (7)  $K_L \to \pi^0 \nu \bar{\nu}$ : We require that the most recent upper limit on the branching fraction from the KOTO experiment at J-PARK be satisfied; see Table I.
- (8)  $K \to \pi \gamma \gamma$ : For these decay modes, we require the dark scalar contribution to be smaller than the measured central values in Table I.
- (9)  $K^{\pm} \rightarrow \mu^{\pm} \nu_{\mu} e^{+} e^{-}$ : The NA48/2 Collaboration has measured  $\mathcal{B}(K^{\pm} \rightarrow \mu^{\pm} \nu_{\mu} e^{+} e^{-}) = (7.81 \pm 0.23) \times 10^{-8}$  [32] in the kinematic region  $m_{e^{+}e^{-}} \geq 140$  MeV. In our model, this decay proceeds through  $K \rightarrow \mu \nu S(\rightarrow e^{+}e^{-})$  where the dark scalar is radiated

off the muon leg. The constraint applies for  $m_S > 140 \,\text{MeV}$ .

B and K meson mixing. The Lagrangian in Eq. (4) also induces meson mixing. The measurement of the mass difference  $\Delta M_{B_s}$  is consistent with the SM prediction. Hence we require the additional contribution to not exceed the uncertainty in the SM expectation. For kaon mixing, the SM prediction suffers from large uncertainties. The long distance contribution is poorly estimated, so we only include the short distance contribution to  $\Delta M_K$  in Table I. The measured value, however, is quite precise and we do not allow the new contribution to  $\Delta M_K$  to exceed the  $1\sigma$  uncertainty in the measurement.

 $(g-2)_{\ell}$ . The dominant contribution to the anomalous magnetic moments of the muon and electron comes from the log enhanced term of the Barr-Zee diagram (see Supplemental Material [50]) which depends on the cutoff scale  $\Lambda$ . We fix  $\Lambda=2$  TeV and require consistency with Eq. (1) within  $1\sigma$ . Because  $\Delta a_e/\Delta a_\mu=m_e^2/m_\mu^2$ , we find  $\Delta a_e\sim {\rm few}\times 10^{-14}$  which is much smaller than the magnitude of the inferred value,  $\mathcal{O}(10^{-13}-10^{-12})$  [65–67].

MiniBooNE. The scattering of a muon neutrino off a nucleus may take place via the dark scalar exchange as shown in Fig. 1. Being heavy, the sterile neutrino produced promptly decays to a light neutrino and the dark scalar, whose subsequent decay to  $e^+e^-$  and  $\gamma\gamma$  may mimic the signal observed in the MiniBooNE experiment. Since MiniBooNE is a Cherenkov detector that cannot distinguish between electrons and photons, two photons or two electrons with a small opening angle can be misidentified as a single electron. The details of the coherent scattering cross sections mediated by the dark scalar can be found in the Supplemental Material [50].

It has been previously shown in Ref. [37] that the dark scalar model is able to explain the excess observed in MiniBooNE data while being consistent with the observations of the CHARM II experiment for  $m_{\nu 4}$  between 400 and 500 MeV. The sterile neutrino has to be heavier than 400 MeV to ensure that less than 70% of the excess events are in the forwardmost bin  $(0.8 < \cos \theta < 1)$  of the angular distribution of electronlike events at MiniBooNE [44]. We compute the coherent and incoherent scattering cross

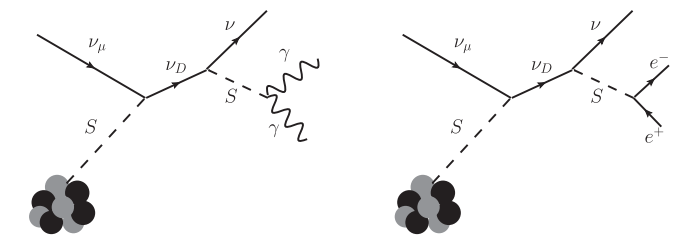


FIG. 1. Dark scalar mediated neutrino-nucleus scattering produces the MiniBooNE signal.

sections at MiniBooNE and CHARM-II and recast the results of Refs. [42,44] for a dark Z' kinetically mixed with the electromagnetic field, to our case. The following constraints are imposed to implement the mapping between the dark Z' model and our model:

(1) In terms of the total scattering cross sections  $\sigma_S$  and  $\sigma_{Z'}$  for the scalar and Z' mediators, respectively, we define

$$\mathcal{R} = \frac{\int \Phi \frac{d\sigma_{S}}{dT} dT dE_{\nu_{\mu}} \times (\mathcal{B}(S \to e^{+}e^{-}) + \mathcal{B}(S \to \gamma\gamma))}{\int \Phi \frac{d\sigma_{Z'}}{dT} dT dE_{\nu_{\mu}} \times \mathcal{B}(Z' \to e^{+}e^{-})},$$
(7)

with the denominator evaluated at the benchmark point  $m_{Z'} = 30 \text{ MeV}$ ,  $\alpha_{Z'} = 0.25$ ,  $\alpha \epsilon^2 = 2 \times 10^{-10}$  of Ref. [42] to explain the MiniBooNE anomaly. The  $\nu_{\mu}$  flux at the Booster Neutrino Beam in the neutrino run [41] is denoted by  $\Phi$ . To reproduce the MiniBooNE signal we require  $0.95 \le \mathcal{R} \le 1.05$ .

(2) The Z' model of Ref. [42], however, is excluded by the CHARM-II constraint in Ref. [44]. To satisfy this constraint, we require

$$\frac{\sigma_{S} \times (\mathcal{B}(S \to e^{+}e^{-}) + \mathcal{B}(S \to \gamma\gamma))}{\sigma_{Z'} \times \mathcal{B}(Z' \to e^{+}e^{-})} < 1 \quad (8)$$

for  $E_{\nu_{\mu}}=20$  GeV, where the denominator is evaluated for the parameter values in Fig. 3 of Ref. [44] with  $|U_{\mu 4}|=10^{-4}$ .

Heavy neutral lepton searches. Several experiments including PS191 [68], NuTeV [69], BEBC [70], FMMF [71], CHARM II [72], T2K [73], NA62 [74], and

MicroBooNE [75] have placed limits on heavy neutral leptons with sufficiently long lifetimes that can reach the detector before decaying into SM particles. However, the limits on  $U_{\mu4}$  from the nonobservation of the decay signal do not apply to our model because  $\nu_4$  has a lifetime of  $\mathcal{O}(0.1)$  ps and decays promptly. The only relevant bound for  $m_{\nu4}$  between 400 and 700 MeV arises from lepton universality:  $|U_{\mu4}\lesssim 0.07$  at the 99% C.L. [76].

Analysis and results. We analyze two cases:  $\kappa \neq 0$  and  $\kappa = 0$ . We find that  $\eta_t \gtrsim 0.005$  is needed to explain the measured branching fraction of  $B^+ \to K^+ \nu \bar{\nu}$ . However, this leads to a correction to the  $K_L \to \pi^0 \nu \bar{\nu}$  branching fraction that violates the upper limit set by the KOTO experiment. To lower the new contribution to  $K_L \to \pi^0 \nu \bar{\nu}$ , a cancellation between the  $\eta_t$ - and  $\eta_c$ -dependent terms in  $g_{sd}$  is required. This is achieved for  $\eta_c \approx -27\eta_t$ . The large  $\eta_c$  does not, however, affect  $g_{bs}$  significantly due to the charm-mass suppression. If nonzero, the coupling  $\kappa$  is primarily constrained by MiniBooNE and g-2 data. Even though the FCNC transitions to invisible final states depend upon the sterile neutrino parameters  $g_D$  and  $U_{\mu4}$ , these are mainly constrained by the  $\nu_u$ -nucleus scattering cross section. For  $\kappa \neq 0$  and  $\kappa = 0$ , we set  $\eta_{\mu} = 0$  for simplicity and scan the other parameters in the following ranges:

$$\begin{split} & \eta_d \in [0,1], \qquad \eta_t \in [0,0.02], \qquad \eta_c \in [-0.5,0], \\ & g_D \in [0,\sqrt{4\pi}], \qquad \kappa \in [0,2] \text{ TeV}^{-1}, \qquad |U_{\mu 4}| \in [0,0.006], \\ & m_S \in [10,150] \text{ MeV}, \qquad m_{\nu 4} \in [400,700] \text{ MeV}. \end{split}$$

For both cases, we choose some benchmark points (BPs) that have interesting consequences for rare *K* and *B* decays.

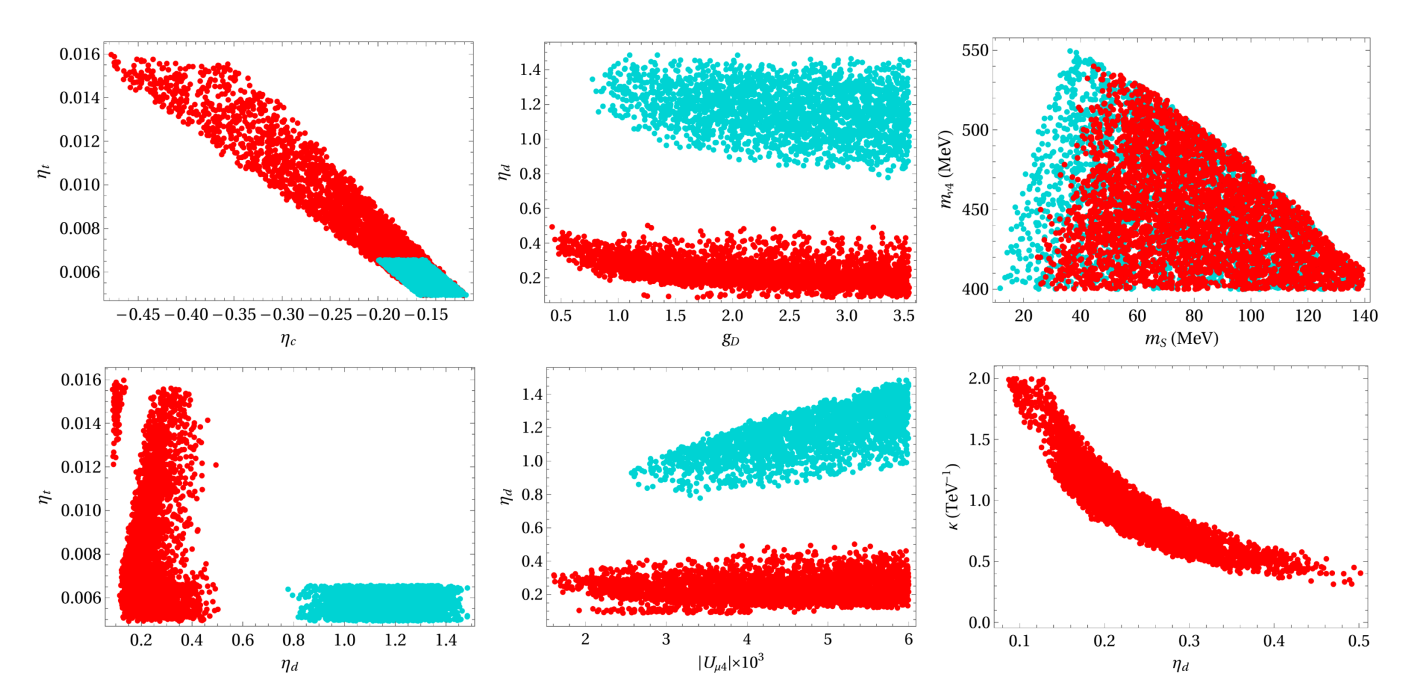


FIG. 2. Allowed regions depicted by red points for  $\kappa \neq 0$  and cyan for  $\kappa = 0$ .

BP	κ (TeV <sup>-1</sup> )	$\eta_d$	$\eta_c$	$\eta_t \times 10^2$	$g_D$	$U_{\mu4} \times 10^3$	$m_S$ (MeV)	$m_{\nu 4} \; ({\rm MeV})$
1	1.22	0.17	-0.13	0.54	2.18	4.86	38	413
2	0.60	0.30	-0.28	1.04	0.94	3.64	93	413
3	1.21	0.21	-0.24	0.84	1.26	5.65	93	432
4	1.03	0.20	-0.14	0.58	3.42	3.25	44	514
5	0.54	0.44	-0.34	1.31	0.52	4.82	138	404
6	0	0.88	-0.13	0.54	3.06	4.73	24	401
7	0	1.40	-0.15	0.63	1.82	5.87	122	429

TABLE II. Benchmark points for  $\kappa \neq 0$  and  $\kappa = 0$  (in which case the g-2 anomaly is unsolved).

TABLE III. Predictions for the benchmark points in Table II.

BP	$\mathcal{B}(S \to \gamma \gamma)$	$\mathcal{B}(S \to \nu \bar{\nu})$	$\mathcal{B}(S \to e^+e^-)$	$\mathcal{B}(K_L \to \pi^0 \nu \bar{\nu})$	$\mathcal{B}(B_s \to \nu \bar{\nu})$	$\mathcal{B}(B \to K^{(*)}\gamma\gamma)$
1	0.093	0.907	$4.26 \times 10^{-5}$	$1.71 \times 10^{-9}$	$5.13 \times 10^{-7}$	$1.3 \times 10^{-6}$
2	0.717	0.282	$7.06 \times 10^{-4}$	$3.61 \times 10^{-11}$	$3.54 \times 10^{-7}$	$3.7 \times 10^{-5}$
3	0.496	0.504	$5.93 \times 10^{-5}$	$9.02 \times 10^{-10}$	$4.14 \times 10^{-7}$	$1.7 \times 10^{-5}$
4	0.165	0.835	$1.10 \times 10^{-4}$	$1.73 \times 10^{-9}$	$1.43 \times 10^{-6}$	$2.65 \times 10^{-6}$
5	0.829	0.170	$9.72 \times 10^{-4}$	$2.04 \times 10^{-10}$	$1.72 \times 10^{-7}$	$6.8 \times 10^{-5}$
6	$4.58 \times 10^{-6}$	0.999	$7.10 \times 10^{-4}$	$1.89 \times 10^{-9}$	$1.01\times10^{-6}$	$6.5 \times 10^{-11}$
7	$3.95 \times 10^{-4}$	0.997	$2.14 \times 10^{-3}$	$2.84 \times 10^{-9}$	$4.86 \times 10^{-7}$	$7.6 \times 10^{-9}$

(a)  $\kappa \neq 0$ : In this case, the dark scalar has a nonzero effective coupling to photons which permits an explanation of the discrepancy in the muon anomalous magnetic moment. The MiniBooNE signal is also enhanced due to the nonzero branching fraction to  $\gamma\gamma$ . In Fig. 2, we show the allowed regions by the red points. As explained above, there is a strong correlation between  $\eta_t$  and  $\eta_c$ . A significant correlation is also observed between  $m_S$  and  $m_{\nu 4}$ . For certain values of  $\eta_d$ , the effective scalar-nucleus coupling responsible for neutrino-nucleus scattering becomes too small to produce a significant scattering cross section due to the fine-tuning between  $\eta_t$  and  $\eta_c$ . Hence we observe gaps in the allowed regions of  $\eta_d$ .

We select five benchmark points, as listed in Table II, that simultaneously explain the  $B^+ \to K^+ \nu \bar{\nu}$ , Mini-BooNE and g-2 anomalies. For each BP we also provide predictions for some important decays in Table III.

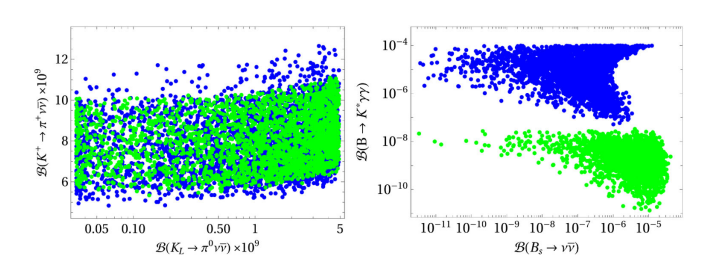


FIG. 3. Branching fractions for kaon and *B* meson decays for  $\kappa \neq 0$  (blue) and  $\kappa = 0$  (green).

(b)  $\kappa=0$ : The allowed regions are shown by the cyan points in Fig. 2. Since the branching of  $S \to \nu \bar{\nu}$  is enhanced in the absence of the  $\gamma \gamma$  mode,  $\eta_t$  is restricted to smaller values by  $\mathcal{B}(B \to K^{(*)}\nu \bar{\nu})$ . The correlation of  $\eta_t$  with  $\eta_c$  remains the same as in the previous case. Further, the contribution to the MiniBooNE signal now only arises from the decay of the dark scalar to  $e^+e^-$ . Hence, larger values of  $\eta_d$  are required to enhance the overall coherent scattering cross section. Smaller values of  $g_D$  and the mixing parameter  $U_{\mu 4}$  are also disfavored. Two benchmark points and predictions for them are provided in Tables II and III, respectively.

Correlations between the branching fractions for kaon and B meson decays are shown in Fig. 3. The branching fraction for  $K^+ \to \pi^+ \nu \bar{\nu}$  is predicted to lie in a quite narrow range. Note that  $K^+ \to \pi^+ \nu \bar{\nu}$  and  $B_s \to \nu \bar{\nu}$  are currently unconstrained for a short-lived dark scalar and sterile neutrino.

Summary. Motivated by the recent Belle II evidence for  $B^+ \to K^+ \nu \bar{\nu}$  which shows a  $\sim 3\sigma$  excess relative to the SM prediction, we explored a new physics explanation of the result in terms of new light states. The new physics contribution to this decay is interpreted as  $B^+ \to K^+ S$ , where S is a light scalar in the mass range  $10 \lesssim m_S/\text{MeV} \lesssim 140$  which then decays to light neutrinos. The interaction of S with light neutrinos occurs via its coupling to a heavy neutral lepton  $\nu_D$  which mixes with the light neutrinos. We demonstrated that our model is consistent with other

measurements and bounds and has interesting predictions for several B and K decays. The excess in electronlike events observed by the MiniBooNE experiment is explained by the upscattering of  $\nu_{\mu}$  to  $\nu_{D}$  which subsequently decays to  $e^+e^-$  and  $\gamma\gamma$  states. Finally, our model can accommodate the recent muon g-2 measurement if S directly couples to photons.

Acknowledgments. A. D. thanks the SLAC National Accelerator Laboratory and the Santa Cruz Institute of Particle Physics for their hospitality during the completion of this work. A. D. is supported in part by the U.S. National Science Foundation under Grant No. PHY-2309937. D. M. is supported in part by the U.S. Department of Energy under Award No. de-sc0010504.

- [1] R. Aaij et al. (LHCb Collaboration), Phys. Rev. Lett. 131, 051803 (2023).
- [2] B. Capdevila, A. Crivellin, and J. Matias, Eur. Phys. J. Special Topics 1, 20 (2023).
- [3] I. Adachi et al. (Belle-II Collaboration), arXiv:2311.14647.
- [4] W. G. Parrott, C. Bouchard, and C. T. H. Davies (HPQCD Collaboration), Phys. Rev. D 107, 014511 (2023); 107, 119903(E) (2023).
- [5] R. Bause, H. Gisbert, and G. Hiller, Phys. Rev. D 109, 015006 (2024).
- [6] L. Allwicher, D. Becirevic, G. Piazza, S. Rosauro-Alcaraz, and O. Sumensari, Phys. Lett. B 848, 138411 (2024).
- [7] P. Athron, R. Martinez, and C. Sierra, arXiv:2308.13426.
- [8] T. Felkl, A. Giri, R. Mohanta, and M. A. Schmidt, Eur. Phys. J. C 83, 1135 (2023).
- [9] X.-G. He, X.-D. Ma, and G. Valencia, arXiv:2309.12741.
- [10] C.-H. Chen and C.-W. Chiang, arXiv:2309.12904.
- [11] F. Abudinén *et al.* (Belle-II Collaboration), Phys. Rev. Lett. 127, 181802 (2021).
- [12] T. E. Browder, N. G. Deshpande, R. Mandal, and R. Sinha, Phys. Rev. D 104, 053007 (2021).
- [13] X. G. He and G. Valencia, Phys. Lett. B 821, 136607 (2021).
- [14] T. Felkl, S. L. Li, and M. A. Schmidt, J. High Energy Phys. 12 (2021) 118.
- [15] X.-G. He, X.-D. Ma, and G. Valencia, J. High Energy Phys. 03 (2023) 037.
- [16] M. Ovchynnikov, M. A. Schmidt, and T. Schwetz, Eur. Phys. J. C 83, 791 (2023).
- [17] P. Asadi, A. Bhattacharya, K. Fraser, S. Homiller, and A. Parikh, J. High Energy Phys. 10 (2023) 069.
- [18] A. J. Buras, J. Girrbach-Noe, C. Niehoff, and D. M. Straub, J. High Energy Phys. 02 (2015) 184.
- [19] J. Grygier et al. (Belle Collaboration), Phys. Rev. D 96, 091101 (2017); 97, 099902(A) (2018).
- [20] O. Lutz *et al.* (Belle Collaboration), Phys. Rev. D **87**, 111103 (2013).
- [21] S. Jäger and J. Martin Camalich, J. High Energy Phys. 05 (2013) 043.
- [22] R. Aaij *et al.* (LHCb Collaboration), J. High Energy Phys. 05 (2013) 159.
- [23] L. Reina, G. Ricciardi, and A. Soni, Phys. Rev. D 56, 5805 (1997).
- [24] D. Dutta *et al.* (Belle Collaboration), Phys. Rev. D 91, 011101 (2015).

- [25] M. Beneke, C. Bobeth, and R. Szafron, Phys. Rev. Lett. 120, 011801 (2018).
- [26] S. Neshatpour, T. Hurth, F. Mahmoudi, and D. Martinez Santos, Springer Proc. Phys. 292, 11 (2023).
- [27] A. J. Buras, D. Buttazzo, J. Girrbach-Noe, and R. Knegjens, J. High Energy Phys. 11 (2015) 033.
- [28] J. K. Ahn *et al.* (KOTO Collaboration), Phys. Rev. Lett. **126**, 121801 (2021).
- [29] G. Buchalla, G. D'Ambrosio, and G. Isidori, Nucl. Phys. B672, 387 (2003).
- [30] A. Alavi-Harati *et al.* (KTeV Collaboration), Phys. Rev. Lett. **93**, 021805 (2004).
- [31] R. L. Workman *et al.* (Particle Data Group), Prog. Theor. Exp. Phys. **2022**, 083C01 (2022).
- [32] G. Khoriauli (NA48/2 Collaboration), J. Phys. Conf. Ser. 800, 012035 (2017).
- [33] L. Di Luzio, M. Kirk, A. Lenz, and T. Rauh, J. High Energy Phys. 12 (2019) 009.
- [34] J. Brod and M. Gorbahn, Phys. Rev. Lett. **108**, 121801 (2012).
- [35] T. Aoyama et al., Phys. Rep. 887, 1 (2020).
- [36] D. P. Aguillard *et al.* (Muon g-2 Collaboration), Phys. Rev. Lett. **131**, 161802 (2023).
- [37] A. Datta, S. Kamali, and D. Marfatia, Phys. Lett. B 807, 135579 (2020).
- [38] B. Batell, N. Lange, D. McKeen, M. Pospelov, and A. Ritz, Phys. Rev. D 95, 075003 (2017).
- [39] A. Datta, J. L. Feng, S. Kamali, and J. Kumar, Phys. Rev. D 101, 035010 (2020).
- [40] J. Liu, N. McGinnis, C. E. M. Wagner, and X.-P. Wang, J. High Energy Phys. 04 (2020) 197.
- [41] A. Aguilar-Arevalo *et al.* (MiniBooNE Collaboration), Phys. Rev. Lett. **121**, 221801 (2018).
- [42] E. Bertuzzo, S. Jana, P. A. Machado, and R. Zukanovich Funchal, Phys. Rev. Lett. **121**, 241801 (2018).
- [43] P. Ballett, S. Pascoli, and M. Ross-Lonergan, Phys. Rev. D **99**, 071701 (2019).
- [44] C. A. Argüelles, M. Hostert, and Y.-D. Tsai, Phys. Rev. Lett. **123**, 261801 (2019).
- [45] P. Vilain *et al.* (CHARM-II Collaboration), Phys. Lett. B **335**, 246 (1994).
- [46] E. Valencia *et al.* (MINERvA Collaboration), Phys. Rev. D 100, 092001 (2019).
- [47] A. M. Abdullahi, J. Hoefken Zink, M. Hostert, D. Massaro, and S. Pascoli, arXiv:2308.02543.

- [48] S. M. Barr and A. Zee, Phys. Rev. Lett. 65, 21 (1990); 65, 2920(E) (1990).
- [49] A. B. Balantekin, A. de Gouvea, and B. Kayser, Phys. Lett. B 789, 488 (2019).
- [50] See Supplemental Material at http://link.aps.org/ supplemental/10.1103/PhysRevD.109.L031701 for relevant formulas, which includes Refs. [51–57].
- [51] M. Carena, I. Low, and C. E. M. Wagner, J. High Energy Phys. 08 (2012) 060.
- [52] A. Crivellin, M. Hoferichter, and M. Procura, Phys. Rev. D 89, 054021 (2014).
- [53] M. Hoferichter, J. Ruiz de Elvira, B. Kubis, and U.-G. Meißner, Phys. Rev. Lett. 115, 092301 (2015).
- [54] P. Junnarkar and A. Walker-Loud, Phys. Rev. D 87, 114510 (2013).
- [55] R. H. Helm, Phys. Rev. 104, 1466 (1956).
- [56] H. Davoudiasl and W. J. Marciano, Phys. Rev. D 98, 075011 (2018).
- [57] J. P. Leveille, Nucl. Phys. **B137**, 63 (1978).
- [58] P. Ball and R. Zwicky, Phys. Rev. D 71, 014015 (2005).
- [59] A. Bharucha, D. M. Straub, and R. Zwicky, J. High Energy Phys. 08 (2016) 098.
- [60] W. J. Marciano and Z. Parsa, Phys. Rev. D 53, R1 (1996).
- [61] A. Lenz, Int. J. Mod. Phys. A 30, 1543005 (2015).
- [62] Y. Aoki et al. (Flavour Lattice Averaging Group (FLAG) Collaboration), Eur. Phys. J. C 82, 869 (2022).

- [63] E. Cortina Gil *et al.* (NA62 Collaboration), J. High Energy Phys. 06 (2021) 093.
- [64] E. Cortina Gil *et al.* (NA62 Collaboration), J. High Energy Phys. 02 (2021) 201.
- [65] D. Hanneke, S. Fogwell, and G. Gabrielse, Phys. Rev. Lett. 100, 120801 (2008).
- [66] R. H. Parker, C. Yu, W. Zhong, B. Estey, and H. Müller, Science 360, 191 (2018).
- [67] T. Aoyama, T. Kinoshita, and M. Nio, Atoms 7, 28 (2019).
- [68] G. Bernardi et al., Phys. Lett. B 203, 332 (1988).
- [69] A. Vaitaitis *et al.* (NuTeV, E815 Collaborations), Phys. Rev. Lett. **83**, 4943 (1999).
- [70] A. M. Cooper-Sarkar *et al.* (WA66 Collaboration), Phys. Lett. **160B**, 207 (1985).
- [71] E. Gallas *et al.* (FMMF Collaboration), Phys. Rev. D **52**, 6 (1995).
- [72] P. Vilain *et al.* (CHARM II Collaboration), Phys. Lett. B 343, 453 (1995).
- [73] K. Abe *et al.* (T2K Collaboration), Phys. Rev. D **100**, 052006 (2019).
- [74] E. Cortina Gil *et al.* (NA62 Collaboration), Phys. Lett. B 816, 136259 (2021).
- [75] P. Abratenko *et al.* (MicroBooNE Collaboration), arXiv:2310.07660.
- [76] A. de Gouvêa and A. Kobach, Phys. Rev. D **93**, 033005 (2016).